Engineering Structures 31 (2009) 2735–2743

Contents lists available at ScienceDirect

Engineering Structures

journal homepage: www.elsevier.com/locate/engstruct

Multidomain finite and discrete elements method for impact analysis of a concrete structure

Jessica Rousseau *, Emmanuel Frangin, Philippe Marin, Laurent Daudeville

3S-R (UJF/INPG/CNRS), DU BP53, 38041 Grenoble Cedex 9, France

ARTICLE INFO

Article history:
Received 27 February 2009
Received in revised form
17 June 2009
Accepted 2 July 2009
Available online 17 July 2009

Keywords:
Discrete elements method
Fast transient dynamics
Concrete
Impact
Spurious waves

ABSTRACT

This article focuses on a formulation for coupling discrete and finite element methods. The efficiency of the discrete element method for studying the fracture of heterogeneous media has been demonstrated, but it is limited by the number of elements. A multidomain analysis is thus proposed in order to reduce the computational effort. The structure is split into two subdomains, in each of which the method is adapted to the behavior of the structure under impact. The DEM is used to model the media close to the impacts. It easily takes into account the discontinuities. The remaining structure is modelled by the FEM. The aims of this paper are to present a method with rotations coupling and to propose a way to reduce spurious wave reflections; it presents an application on a rock impact on a concrete slab.

1. Introduction

Particular attention must be paid during the design of certain civil engineering structures in order to predict their response under severe dynamic loading. One or several impacts of a projectile like an aircraft or a missile on a sensitive concrete structure may have disastrous consequences — for example, if the impact provides perforation on structure that has some protective functions (airtightness). This paper deals with a new numerical method to simulate an impact on a concrete structure. The structure is divided into two subdomains. On each of them, the best fit method is used. The approach uses a coupling between the Discrete Element (DE) Method and the Finite Element (FE) Method. In the vicinity of the impact, where important non-linear phenomena occur, the medium will be modelled by means of discrete elements. Far from this area, the response of the structure may be considered as linear elastic, and this complementary subdomain is modelled with the FE method.

Contrary to non-linear continuum methods [1], the DE method easily takes into account discontinuous phenomena. Our approach uses rigid sphere interactions, such as were used by Cundall [2]. The DE method is used in the impacted subdomain. These methods have been used first to model the behavior of granular materials, but also provide very accurate results for cohesive materials like concrete [3]. The studies of Camborde in 2D [4] or Rousseau et al. in 3D [5] have demonstrated the efficiency of such a discrete approach to deal with impact problems on reinforced concrete structures. They have also pointed out that such a method is limited to small structures because of the computation cost. The use of the FE method far from the impacted area is a way to reduce this limitation. Meshing softwares drastically reduce the time of modelling and the calculation may be faster than with a full DE approach because of the facility to handle different discretization sizes. Moreover the global behavior shows that the DE method is not needed on the whole structure. The aim of the coupled method is the prediction of both the local damage or the penetration of the projectile, and the global displacement of the structure.

Many studies deal with combined continuum/discrete methods, mainly with molecular dynamics and FE methods for the analysis of the fracture process at the atomic scale. A large review of such methods is proposed in Li and Liu [6], Rabczuk et al. [7]. Many applications have been carried out on concrete structures; in static by Azevedo et al. [8], Cusatis et al. [9] for the analysis of the fracturing process in heterogeneous materials; in transient analyses, and Onate and Rojek [10] studies the contact between FE and DE, Bicanic et al. [11] proposed a combined approach where the whole structure is modelled with FE which are disconnected and transformed to DE, depending on a stress criterion. Concerning the coupling between DE an FE, the works of Xiao and Belytschko [12] proposed a coupling using a bridging domain. Ben Dhia and Rateau [13] proposed the Arlequin method also based on a bridging domain with a weak formulation of the kinematic relations. In Xiao and Belytschko [12], the authors present some particular numerical simplification that improves the computational

* Corresponding author. Tel.: +33 4 56 52 86 49; fax: +33 4 76 82 70 00.
E-mail address: jessica.rousseau@hmg.inpg.fr (J. Rousseau).

0141-0296/$ – see front matter © 2009 Elsevier Ltd. All rights reserved.
doi:10.1016/j.engstruct.2009.07.001

Nomenclature

$\overrightarrow{d_j}$	vector of the three displacements of the DE j
$\overrightarrow{\omega_j}$	vector of the three rotations of the DE j
$\overrightarrow{u_i}$	vector of the three displacement of FE node i
n_f	Number of FE nodes
n_d	Number of DE nodes
n_{fb}	Number of FE nodes in the bridging domain
n_{db}	Number of DE nodes in the bridging domain
n_b	Number of FE layers in the bridging domain
α_i	Bridging parameter for the FE node i
β_j	Bridging parameter for the DE j
r	Relaxation parameter
M_j	Mass of the DE j
J_j	Inertia of the DE j
m_i	Mass of the FE node i
$\overrightarrow{Fg_i}$	Generalized force vector on FE node i
$\overrightarrow{F_j^{tot}}$	Total force applied to DE j
$\overrightarrow{C_j^{tot}}$	Total couple applied to DE j
$\overrightarrow{\lambda^d}$	Lagrange multipliers related to displacement coupling
$\overrightarrow{\lambda^\omega}$	Lagrange multipliers related to rotation coupling
$\overline{\overline{k}}$	Displacement coupling matrix
$\overline{\overline{h}}$	Rotation coupling matrix

time and decreases the spurious wave reflection given by the interface.

The originality of our method is that we have to take into account the rotations of DE. Moreover, the numerical simplification discussed before does not strongly attenuate the high frequencies' reflection. We propose a new way to deal with the temporal DE boundary conditions. We introduce a temporal relaxation of the kinematic relations. This method strongly attenuates the spurious reflection due to different size discretization between the two methods. This method is equivalent to the use of the penalty method with a penalty parameter adapted to each degree of freedom (dof).

The discrete model and the main difficulties of coupling are first presented. Details of the coupling method are given, and a special emphasis on spurious wave reflections is carried out. Then we present our method to attenuate spurious reflections. It uses a relaxation of the Lagrange multipliers associated to the kinematic continuity. At the end, DE and DE/FE simulations of an impact on a concrete slab are compared.

2. Model description

The problem deals with fast transient dynamics in two subdomains of a concrete structure. One subdomain is modelled with DE, the other one with FE. This separation is done *a priori* from an estimation of the size of the damageable area. This step may be estimated from experimental analyses on a concrete slab [14] or from design rules (Eurocode 2, [15]). It depends on the kind of impact (soft [16], hard [17]), the geometry of the structure and, of course, the velocity of the impactor. Lots of experiments are accessible to estimate the size of the damageable part of the structure, so as to know the minimum size of the DE model. Moreover, we can check *a posteriori* that the stresses in FE domain stay in the elastic domain of the media. Another way is to verify that DE of the bridging domain have stayed in the elastic domain.

2.1. Discrete model

The domain, where discontinuities and non-linearities occur, is modelled with the DE method. Previous studies have demonstrated the efficiency of this approach to analyze structures under high deformation or many non linearities, in 2D [18] or 3D [19], in statics [9] or dynamics [20]. Our model is close to the one proposed by Cundall and Stack [2]. The heterogeneous medium is modelled by randomly positioned rigid spheres of different radii in interaction, link or contact. To represent the cohesive property of concrete, two elements can interact without being in contact. In [21], Hentz et al. presents a large description of the DE model. A modified Mohr–Coulomb criterion associated with softening is used to model the cohesive behavior of the material, and a classical friction constitutive behavior is used between the elements in contact. The material is modelled at a macro-scale, with the size of the DE being larger than the aggregate size. Nevertheless, the DE size will be as small as possible with respect to the computational time. Finally, an identification process is used to ensure that the model is predictive [21].

The DE degrees of freedom (dof) are three displacements and three rotations, so three more than the node of the FE model.

More details about complete model of the interaction laws and damage are available in Rousseau et al. [22] or Hentz et al. [21].

2.2. Continuum model

Far from the impacted area, the structure is modelled with the FE method under the small perturbation assumption. This assumption might be seen as a main constraint of the model, but the FE stresses can be used as an error indicator on the assumption, and it is still possible to enlarge the DE domain with, of course, a loss on the computation time or on the discretization size. Another indicator can be the damage of DE next to FE domain. In this paper, we focus on simulation with localized damage. The FE method is used to reduce the times of modelling (meshing) and computation by reducing the number of DE. The characteristic size of FE is a function of the structure size and its geometry. The FE size is much larger than the DE size (the ratio of discretization size is about 5).

2.3. Main difficulties of the coupling

The coupling can be realized by means of an edge to edge method or with a bridging domain [12] where energy is taken as a linear combination of each model by using a bridging parameter. In our case, due to the random positioning of DE, this model naturally takes into account the non regular boundaries. In some cases, particular treatment of the bridging domain is a way to reduce reflections that appear due to the model.

The numbers of dof in each model are not the same. In addition to the three displacements, the DE node also has three dof in rotation. The kinematic coupling of DE dof and FE dof must take into account the rotation continuity. Coupling rotations decreased error on discrete rotations, but had a slight influence on the displacements. For example, in a 3D case where the theoretical displacements and rotations were known, we obtained the following errors: 5% on discrete rotations and less than 0.5% on displacements. Numerical and physical experiments [23] show that, under the small perturbation assumption, the discrete rotation is the rigid rotation linked to the antisymmetric part of the displacement gradient. In the continuum model, under small strain, the displacement of N in the neighborhood of M is given by:

$$\vec{U}(N) \cong \vec{U}(M) + \overline{\overline{\varepsilon}}(M)\,\overrightarrow{MN} + \overline{\overline{\omega}}\,\overrightarrow{MN}$$
$$\text{with } \overline{\overline{\omega}} = \frac{1}{2}\left(\overline{\overline{\overrightarrow{grad}}}\,\vec{U} - \overline{\overline{\overrightarrow{grad}}}^{\mathrm{T}}\,\vec{U}\right). \quad (1)$$

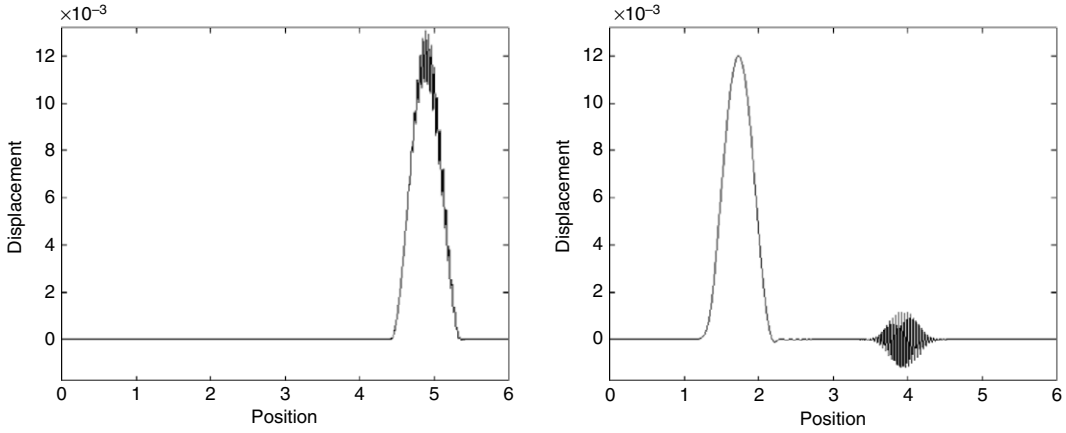

Fig. 1. Wave in DE model (left) and Spurious wave (right).

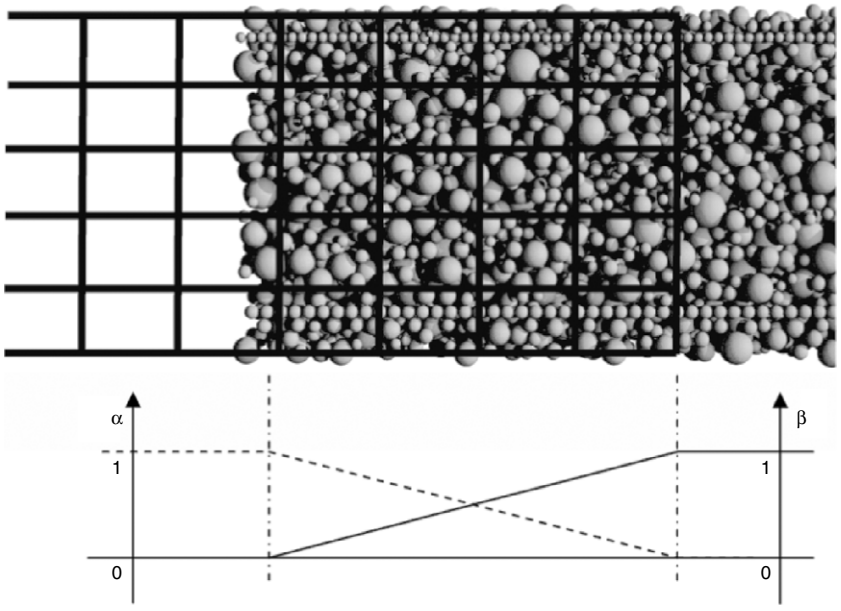

Fig. 2. Bridging domain and bridging parameter.

The displacement is written as the sum of a rigid body translation, one part due to strain and one due to rotation.

Another difficulty is that the discretization size is not uniform between the two models. The discretization size has a direct effect on the frequency range of the model. It is a key point in transient dynamics. A high frequency wave propagating from the DE model (fine) to the FE model (coarse) will introduce spurious wave reflections if the frequency is greater than the cut-off frequency of the FE model. The impact on reinforced concrete structure leads to a large frequency range. The experiments of Zineddin and Krauthammer [24] present high frequencies.

Fig. 1 shows an example of this reflection at the interface between the two models. It is a 1D model, where half of the structure (left) is modelled with coarse regular FE, and the other half with a fine DE model. The displacement wave is generated in displacement on the right hand boundary of the DE model by a sum of two low and high frequencies. The low frequency is transmitted, but the high frequency is fully reflected. This spurious reflection has to be suppressed in order to predict the correct response of the structure in the impacted area. It is to be noticed that such a problem also appears by replacing the fine DE model by a fine FE model. It is only due to the size of the coarse mesh that cannot represent short wave length.

3. The coupled method

3.1. Methods

The proposed method uses a bridging domain in which the Hamiltonian is taken as a linear combination of discrete and continuum Hamiltonians. The bridging parameters α and $1-\alpha$ are introduced respectively for FE and DE. They vary linearly, between 0 and 1, inside the bridging domain, and they are constant in the thickness of the structure. They are introduced to ensure the continuity of the energetic ration between DE model and FE model. The size of the bridging domain is defined by the parameter n_b corresponding to the number of FE layers in the bridging domain. Fig. 2 presents variations of bridging parameters for a bridging domain where $n_b = 4$. The Eq. (2) defines the expression of the Hamiltonian.

$$H = \alpha H_{FE} + (1-\alpha) H_{DE}. \tag{2}$$

In the bridging domain, the DE dof are linked to FE dof through the coupling relations, which can be written at the global scale by (3) and (4) or at the node scale by (5) and (6). Here, we separate translation $\vec{d}_b$ and rotation $\vec{\omega}_b$ dof of the discrete elements. Finally, there are as many coupling relations as DE dof in the bridging

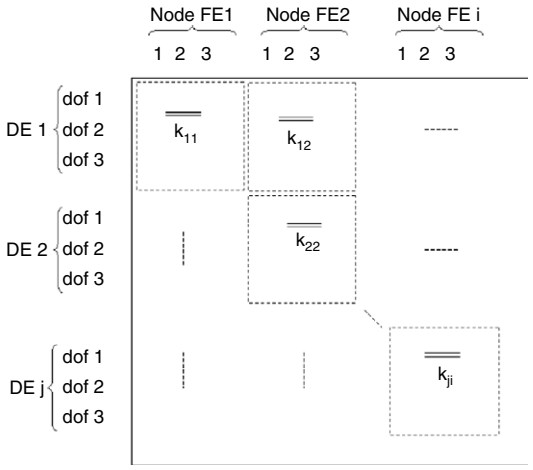

Fig. 3. Description of the coupling matrices.

domain. These coupling relations strictly ensure the displacement continuity. The DE domain is chosen in the vicinity of the impact, and large enough to assume that all dissipative phenomena are concentrated in the DE domain. Thus, no severe damage is assumed to occur in the the bridging domain.

$$\vec{d}_b = \bar{\bar{k}}\,\overrightarrow{u_b} \tag{3}$$

$$\overrightarrow{\omega_b} = \bar{\bar{h}}\,\overrightarrow{u_b} \tag{4}$$

$$\forall j \le n_{db} \quad \overrightarrow{d_j} = \sum_{i=1}^{n_{fb}} \overline{\overline{k_{ji}}}\,\overrightarrow{u_i} \tag{5}$$

$$\forall j \le n_{db} \quad \overrightarrow{\omega_j} = \sum_{i=1}^{n_{fb}} \overline{\overline{h_{ji}}}\,\overrightarrow{u_i}\,. \tag{6}$$

$\overline{\overline{k_{ji}}}$ and $\overline{\overline{h_{ji}}}$ are submatrices of $\bar{\bar{k}}$ and $\bar{\bar{h}}$, relative to FE node i and DE node j (Fig. 3). The Eq. (6) is derived from the relation (1) between the rotation and the antisymmetric part of continuum displacement.

The solution minimizes the Hamiltonian in each domain by the introduction of coupling relations in the bridging domain that use Lagrange multipliers. The minimization of (7) gives local equations.

$$H_g\left(\overrightarrow{d}, \overrightarrow{\omega}, \overrightarrow{u}, \overrightarrow{\lambda^d}, \overrightarrow{\lambda^\omega}\right) = H\left(\overrightarrow{d}, \overrightarrow{\omega}, \overrightarrow{u}\right) + \overrightarrow{\lambda^d}\left(\overrightarrow{d_b} - \bar{\bar{k}}\,\overrightarrow{u_b}\right) + \overrightarrow{\lambda^\omega}\left(\overrightarrow{\omega}_b - \bar{\bar{h}}\,\overrightarrow{u_b}\right). \tag{7}$$

- Local equations of DE node j:

$$M_j \ddot{\vec{d}}_j = \overrightarrow{F_j^{tot}} \tag{8}$$

$$J_j \ddot{\vec{\omega}}_j = \overrightarrow{C_j^{tot}} \tag{9}$$

- Local equations of FE node i:

$$m_i \ddot{\vec{u}}_i = \overrightarrow{Fg}_i \tag{10}$$

- In the bridging domain:

$$\forall j \le n_{db} \quad \beta_j M_j \ddot{\vec{d}}_j = \beta_j \overrightarrow{F_j^{tot}} + \overrightarrow{\lambda_j^d} \quad \text{with } \beta_j = 1 - \alpha_j \tag{11}$$

$$\forall j \le n_{db} \quad \beta_j J_j \ddot{\vec{\omega}}_j = \beta_j \overrightarrow{C_j^{tot}} + \overrightarrow{\lambda_j^\omega} \tag{12}$$

$$\forall i \le n_{fb} \quad \alpha_i m_i \ddot{\vec{u}}_i = \alpha_i \overrightarrow{Fg_i} + \sum_{l=1}^{n_{db}} \left(\overline{\overline{k_{li}}}\,\overrightarrow{\lambda_l^d} + \overline{\overline{h_{li}}}\,\overrightarrow{\lambda_l^\omega}\right). \tag{13}$$

3.2. Algorithm

The time discretization is performed with the central difference method.

$$U(t + \Delta t) = 2U(t) - U(t - \Delta t) + \Delta t^2 \ddot{U}(t)\,. \tag{14}$$

The dof at time $t + \Delta t$ can be expressed by:

$$\overrightarrow{d_j}(t + \Delta t) = 2\overrightarrow{d_j}(t) - \overrightarrow{d_j}(t - \Delta t) + \frac{\Delta t^2}{M_j}\left(\overrightarrow{F_j^{tot}} + \frac{\overrightarrow{\lambda_j^d}}{\beta_j}\right) \tag{15}$$

$$\overrightarrow{\omega_j}(t + \Delta t) = 2\overrightarrow{\omega_j}(t) - \overrightarrow{\omega_j}(t - \Delta t) + \frac{\Delta t^2}{J_j}\left(\overrightarrow{C_j^{tot}} + \frac{\overrightarrow{\lambda_j^\omega}}{\beta_j}\right) \tag{16}$$

$$\overrightarrow{u_i}(t + \Delta t) = 2\overrightarrow{u_i}(t) - u_i(t - \Delta t) + \frac{\Delta t^2}{m_i}\vec{F}g_i + \frac{\Delta t^2}{\alpha_i m_i}\left(\sum_{l=1}^{n_{db}} \overline{\overline{k_{li}}}^{\mathrm{T}}\overrightarrow{\lambda_l^d} + \sum_{l=1}^{n_{db}} \overline{\overline{h_{li}}}^{\mathrm{T}}\overrightarrow{\lambda_l^\omega}\right). \tag{17}$$

As a first step, a provisional value of the dof is computed without taking into account Lagrange multipliers.

$$\tilde{\overrightarrow{d_j}}(t + \Delta t) = 2\overrightarrow{d_j}(t) - \overrightarrow{d_j}(t - \Delta t) + \frac{\Delta t^2}{M_j}\overrightarrow{F_j^{tot}} \tag{18}$$

$$\tilde{\overrightarrow{\omega_j}}(t + \Delta t) = 2\overrightarrow{\omega_j}(t) - \overrightarrow{\omega_j}(t - \Delta t) + \frac{\Delta t^2}{J_j}\overrightarrow{C_j^{tot}} \tag{19}$$

$$\tilde{\overrightarrow{u_i}}(t + \Delta t) = 2\overrightarrow{u_i}(t) - \overrightarrow{u_i}(t - \Delta t) + \frac{\Delta t^2}{m_i}\overrightarrow{Fg_i}. \tag{20}$$

The dof $\vec{d}_j, \vec{\omega}_j, \vec{u}_i$ at $t + \Delta t$ have to verify the coupling relations (5) and (6). This constraint leads to the computation of Lagrange multipliers with the expressions:

$$\begin{aligned} \vec{g}_j^d &= \tilde{\vec{d}}_j(t + \Delta t) - \sum_{i=1}^{n_{fb}} \overline{\overline{k_{ji}}}\,\tilde{\vec{u}}_i(t + \Delta t) \\ \vec{g}_j^d &= \Delta t^2\left(-\frac{\overrightarrow{\lambda_j^d}}{\beta_j M_j} - \sum_{i=1}^{n_{fb}} \overline{\overline{k_{ji}}}\left(\sum_{l=1}^{n_{db}} \frac{\overline{\overline{k_{li}}}\,\overrightarrow{\lambda_l^d} + \overline{\overline{h_{li}}}\,\overrightarrow{\lambda_l^\omega}}{\alpha_i m_i}\right)\right) \end{aligned} \tag{21}$$

$$\begin{aligned} \vec{g}_j^\omega &= \tilde{\vec{\omega}}_j(t + \Delta t) - \sum_{i=1}^{n_{fb}} \overline{\overline{h_{ji}}}\,\tilde{\vec{u}}_i(t + \Delta t) \\ &= \Delta t^2\left(-\frac{\overrightarrow{\lambda_j^\omega}}{\beta_j J_j} - \sum_{i=1}^{n_{fb}} \overline{\overline{h_{ji}}}\left(\sum_{l=1}^{n_{db}} \frac{\overline{\overline{k_{li}}}\,\overrightarrow{\lambda_l^d} + \overline{\overline{h_{li}}}\,\overrightarrow{\lambda_l^\omega}}{\alpha_i m_i}\right)\right). \end{aligned} \tag{22}$$

These expressions can be written in a matrix form:

$$\vec{g}^d = \bar{\bar{A}}\vec{\lambda}^d + \bar{\bar{B}}\vec{\lambda}^\omega \tag{23}$$

$$\vec{g}^\omega = \bar{\bar{C}}\vec{\lambda}^d + \bar{\bar{D}}\vec{\lambda}^\omega. \tag{24}$$

The matrices are:

$$\bar{\bar{A}}_{jl} = -\frac{\Delta t^2}{\beta_j M_j}\overline{\overline{\delta_{jl}}} - \Delta t^2 \sum_{p=1}^{n_{fb}} \frac{\overline{\overline{k_{jp}}}\;\overline{\overline{k_{lp}}}^{\mathrm{T}}}{\alpha_p m_p} \tag{25}$$

$$\bar{\bar{B}}_{jl} = -\Delta t^2 \sum_{p=1}^{n_{fb}} \frac{\overline{\overline{k_{jp}}}\;\overline{\overline{h_{lp}}}^{\mathrm{T}}}{\alpha_p m_p} \tag{26}$$

$$\overline{\overline{C}}_{jl} = -\Delta t^2 \sum_{p=1}^{n_{fb}} \frac{\overline{\overline{h_{jp}}}\,\overline{\overline{k_{lp}}}^{\mathrm{T}}}{\alpha_p m_p} \tag{27}$$

$$\overline{\overline{D}}_{jl} = -\frac{\Delta t^2}{\beta_j J_j}\overline{\overline{\delta}}_{jl} - \Delta t^2 \sum_{p=1}^{n_{fb}} \frac{\overline{\overline{h_{jp}}}\,\overline{\overline{h_{lp}}}^{\mathrm{T}}}{\alpha_p m_p}. \tag{28}$$

The resolution of this matrix system gives the values of Lagrange multipliers. The displacements and rotations of each node are then computed with the relations (15)–(17).

Note that it is also possible to write this algorithm by means of a more classical formulation based on velocities (Casadei and Halleux [25] and Key [26]).

Also note that, in the description of the terms of the matrix, the coefficients α and β are at denominator. Their value cannot be null and therefore we chose a minimum value equal to 0.01 for these parameters because it gives correct results without modifying the critical time step imposed by the stability condition.

3.3. Numerical simplifications

The previous algorithm rigorously respects the coupling relations. Some simplifications can be realized to reduce the computation time. The size of the system to solve is proportional to the number of DE in the bridging domain, which can be large in three dimensions. Moreover, the analysis of the previous matrices shows the predominance of $\overline{\overline{A}}$ and $\overline{\overline{D}}$ in front of $\overline{\overline{B}}$ and $\overline{\overline{C}}$. Lagrange multipliers are then computed without taking into account matrices $\overline{\overline{B}}$ and $\overline{\overline{C}}$.

Then, the values of the diagonal terms of $\overline{\overline{A}}$ and $\overline{\overline{D}}$ are prevailing in relation to the other ones, so the simplifications proposed by Xiao and Belytschko in [12] are used. The matrix is replaced by a diagonal matrix where the value of each diagonal term is equal to the sum of terms of the corresponding line. This numerical simplification can be considered as a way to relax the strict coupling relations (5) and (6). It has two advantages: firstly, the computation time is reduced, and secondly, the spurious wave reflection is slightly reduced (Chapter 4).

We will demonstrate, in the following paragraph, that this simplification is equivalent to the use of the penalty method with a penalty parameter adapted to each dof. Moreover, this parameter is computed automatically. We will define $\overline{\overline{\backslash A}}$ as the diagonalized matrix of $\overline{\overline{A}}$. $\overline{\overline{\backslash A}}_{jj}$ is the diagonal submatrix related to the DE node j. The same notation is used for $\overline{\overline{D}}$.

3.4. Equivalence with the penalty method

The equivalence between the previous method with diagonal matrices and the penalty method is shown on the local equation of DE displacement. The same demonstration can be carried out for the DE rotation. The update of DE displacement dof is obtained by:

$$\overrightarrow{d_j}\,(t+\Delta t) = 2\overrightarrow{d_j}\,(t) - \overrightarrow{d_j}\,(t-\Delta t) + \frac{\Delta t^2}{M_j}\left(\overrightarrow{F_j^{tot}} + \frac{\overline{\overline{\backslash A_{jj}}}^{-1}\overrightarrow{g_j^d}}{\beta_j}\right). \tag{29}$$

On the other hand, the generalized penalty method is obtained by minimizing the Hamiltonian expressed by:

$$H\left(\overrightarrow{d}, \overrightarrow{\omega}, \overrightarrow{u}\right) + \left(\overrightarrow{d_b} - \overline{\overline{k}}\,\overrightarrow{u_b}\right)^{\mathrm{T}} \overline{\overline{p^d}} \left(\overrightarrow{d_b} - \overline{\overline{k}}\,\overrightarrow{u_b}\right) + \left(\overrightarrow{\omega_b} - \overline{\overline{h}}\,\overrightarrow{u_b}\right)^{\mathrm{T}} \overline{\overline{p^\omega}} \left(\overrightarrow{\omega_b} - \overline{\overline{h}}\,\overrightarrow{u_b}\right) \tag{30}$$

where $\overline{\overline{p_d}}$ and $\overline{\overline{p_\omega}}$ in the general case two symmetric positive-defined matrices. In this demonstration, we use, as it is most often done, two diagonal matrices. The DE displacement local equation is obtained with the penalty method:

$$\beta_j m_j \overrightarrow{\ddot{d}_j} = \beta_j \overrightarrow{F_j^{tot}} + \overline{\overline{p_{jj}^d}}\left(\overrightarrow{d_j} - \sum_{i=1}^{n_{fb}} \overline{\overline{k_{ji}}}\,\overrightarrow{u_i}\right). \tag{31}$$

With the central difference scheme:

$$\overrightarrow{d_j}\,(t+\Delta t) = 2\overrightarrow{d_j}\,(t) - \overrightarrow{d_j}\,(t-\Delta t) + \frac{\Delta t^2}{M_j}\left(\overrightarrow{F_j^{tot}} + \frac{\overline{\overline{p_{jj}^d}}\left(\overrightarrow{d_j} - \sum_{i=1}^{n_{fb}} \overline{\overline{k_{ji}}}\,\overrightarrow{u_i}\right)}{\beta_j}\right). \tag{32}$$

With our notation, $\left(\overrightarrow{d_j} - \sum_{i=1}^{n_{fb}} \overline{\overline{k_{ji}}}\,\overrightarrow{u_i}\right)$ is equal to $\vec{g}_j^d$. The Eqs. (29) and (32) are then equivalent if we choose $\overline{\overline{p_{jj}^d}} = \overline{\overline{\backslash A_{jj}}}^{-1}$. The generalization to the DE rotation is easily accomplished. Each coupling relation has its own penalty parameter that is computed automatically.

4. Wave propagations

4.1. Reflections of the high frequency waves

In fast transient dynamics analyses, the discretization size gives the frequency range of the model. To be correctly described, a wave must have a length more than 10 times longer than the discretization size for both of our methods (DE or FE models). Some small waves can propagate in the fine DE model, but cannot be described in the coarse FE model. They are reflected as soon as they enter the bridging domain, which appears for these waves as a rigid body (Fig. 1). Those spurious reflective waves have no physical sense and, to keep a predictable model, they have to be deleted or at least attenuated.

To attenuate this spurious wave, we propose to make numerical simplifications in the Lagrange method. We will see that such simplifications have a beneficial effect on the spurious wave. The presented method with diagonalized matrices slightly reduces the reflected wave (Fig. 4). But, on the contrary of Xiao's applications [12], the attenuation of the reflected waves are not enough. It depends of the frequency range and of the size of discretization. To improve this transient dynamic phenomenon, we introduce a relaxation parameter of the kinematic constraints. It introduces a temporal freedom on DE dof.

4.2. Attenuation with relaxation

With the Lagrange multipliers method, the kinematic constraints are rigorously satisfied. Thus, the method gives the same results as a direct kinematic coupling, and full spurious reflections occur. In fact, all the DE dof are defined from the coarse discretization. The relaxation reduces the value of the Lagrange multipliers, and the coupling relations are not strictly respected. During the update step of dof, Lagrange multipliers are divided by a relaxation parameter, r.

$$\overrightarrow{d_j}\,(t+\Delta t) = 2\overrightarrow{d_j}\,(t) - \overrightarrow{d_j}\,(t-\Delta t) + \frac{\Delta t^2}{M_j}\left(\overrightarrow{F_j^{tot}} + \frac{\overrightarrow{\lambda_j^d}}{\beta_j r}\right) \tag{33}$$

$$\overrightarrow{\omega_j}\,(t+\Delta t) = 2\overrightarrow{\omega_j}\,(t) - \overrightarrow{\omega_j}\,(t-\Delta t) + \frac{\Delta t^2}{J_j}\left(\overrightarrow{C_j^{tot}} + \frac{\overrightarrow{\lambda_j^\omega}}{\beta_j r}\right) \tag{34}$$

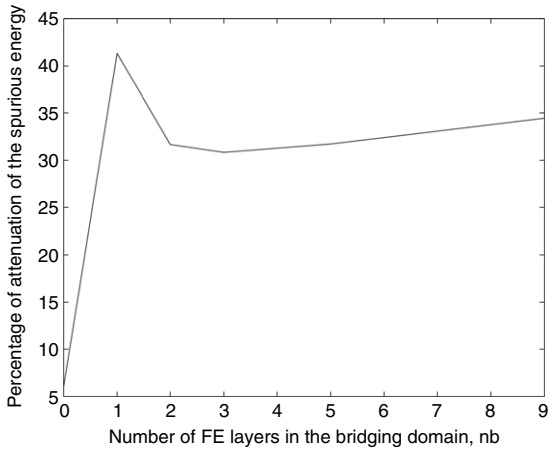

Fig. 4. Influence of diagonal matrices.

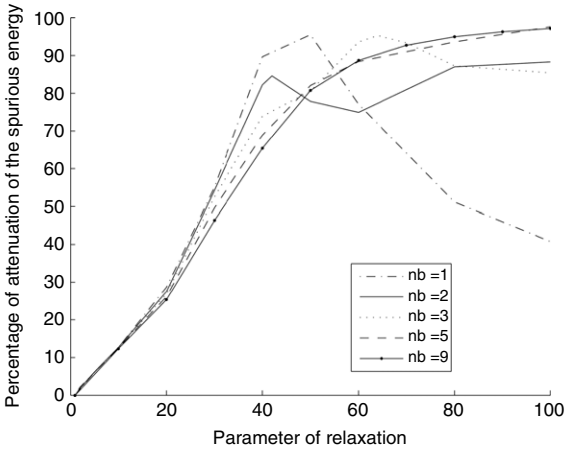

Fig. 5. Influence of the relaxation parameter.

$$\overrightarrow{u_i}\,(t+\Delta t) = 2\overrightarrow{u_i}\,(t) - \overrightarrow{u_i}\,(t-\Delta t) + \frac{\Delta t^2}{m_i}\overrightarrow{Fg_i} + \frac{\Delta t^2}{\alpha_i m_i}\left(\sum_{l=1}^{n_{db}} \frac{\overline{\overline{k_{li}}}^{\mathrm{T}}\overrightarrow{\lambda_l^d} + \overline{\overline{h_{li}}}^{\mathrm{T}}\overrightarrow{\lambda_l^\omega}}{r}\right). \quad (35)$$

By adding this temporal freedom on the kinematic coupling, the spurious reflected waves are strongly attenuated. The next figures show, using a 1D example, the efficiency of the proposed method, with or without diagonal values, and with or without relaxation. The percentage attenuation of the spurious reflected energy for the different methods are compared. The reference is defined with the full Lagrange method without diagonal matrices and without relaxation.

Fig. 4 shows the influence of diagonal matrices. The simplification, in addition to the time reduction, is a way to reduce the spurious reflected energy. As soon as the bridging domain is defined with one FE layer, the energy attenuation is greater than 30%.

Fig. 5 shows the attenuation for many FE layers and many values of relaxation. The relaxation drastically reduces the reflection. For every FE layer, about 99% attenuation can be reached.

Finally, Fig. 6 describes the attenuation for our proposed method (relaxation, diagonalized matrices). For at least two FE layers, the reflection attenuation is greater than 80% and, with three or more FE layers, the energy contained in the reflected wave is fully attenuated for a large range of values of the relaxation parameter.

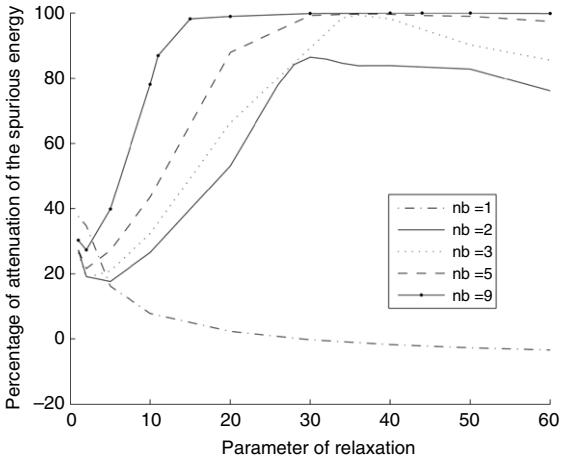

Fig. 6. Influence of diagonal matrices and relaxation.

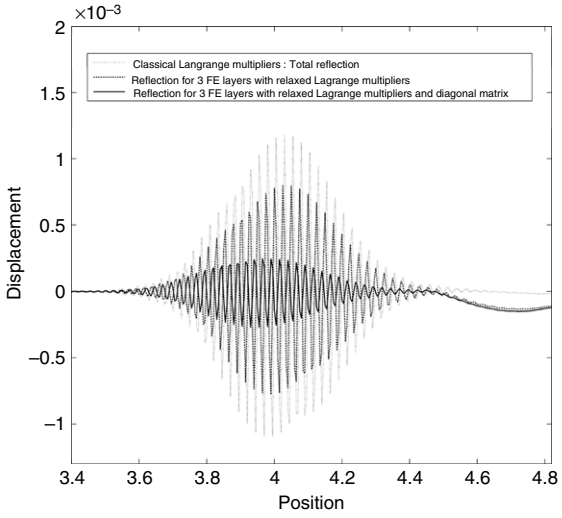

Fig. 7. Spurious reflective wave for each model.

Fig. 7 shows, in detail, the form of the spurious wave for each method. This wave has not disappeared, but it has negligible energy.

Any of the previous methods have significant influences on the propagation of the low frequency wave. The variations of the transmitted wave energy do not exceed 1%. Moreover, as soon as the number of FE layers is enough, the attenuation is effective for a large range of relaxation. A compound must be found between small DE model and attenuation. An efficient method would be to use 3 FE layers with a parameter of relaxation about 10 times the ratio of discretization. For example, a relaxation parameter between 25 and 35 would give correct attenuation for a discretization ratio of 5 and more than two coupling layers (Fig. 6).This study on a one dimensional model will be used for three dimension simulation. The previous tests (Fig. 4 to Fig. 7) have been realized in 1D to have more explicit results without the deterioration of the wave form along the structure due to the many reflections on each face of the solid. But some numerical experiments have been realized in order to verify that the influence of the relaxation is similar in 1D and 3D. They showed that the 1D conclusions were usable for 3D simulations.

5. Impact on a concrete slab

In this part, we wish to compare results from a full discrete elements formulation with the combined finite/discrete elements

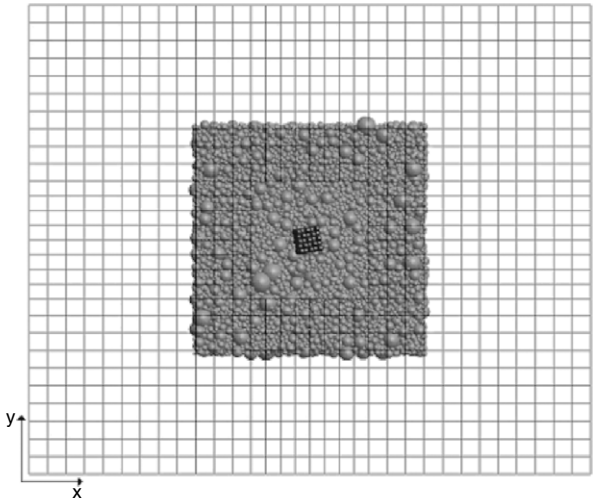

Fig. 8. Combined FE/DE model.

method, with a focus on precision and computation time. The aim of this part is to validate the coupled approach. The proposed method is applied to the simulation of a rock impact on a concrete slab. To make it more realistic, we used data from a real test; more information can be found in Hentz et al. [27]. Simulation results are analyzed in terms of displacement and damage. The computation times are compared for a full DE model and a combined FE/DE model using three FE layers and a relaxation parameter equal to 35. All the simulations were computed with the same computer.

Fig. 8 defines the geometrical model. It consists of a concrete slab (2.5 × 2 × 0.28 m). The characteristics of the concrete are: Young's Modulus of 31 GPa and a compressive strength of 31 MPa. Two opposite faces are restrained on the direction perpendicular to the medium slab plane. The slab is impacted by a concrete cubic block of DE (30 cm side). The figure shows the ratio of discretization between DE and FE equal to three in the plane of the slab, and around one and half in the normal direction, to have enough FE to represent correctly the behavior of the slab in the FE part.

The velocity of the impactor is 40 m/s. The contact between the impactor and the slab is treated by means of the contact laws developed for DE. More details about this can be found in Hentz et al. [21] or Rousseau et al. [22].

Fig. 9 presents comparisons between both methods. The first two figures concern the DE displacement in the DE domain, the next one is DE displacement in the bridging domain and the last one is the displacement comparison of a DE node with the nearest FE node. The predictions of maximum displacements of both models are similar, and the time response is globally the same for the two models.

The combined model is also efficient in describing the damage in the vicinity of the impacted zone. In Fig. 10, damages obtained

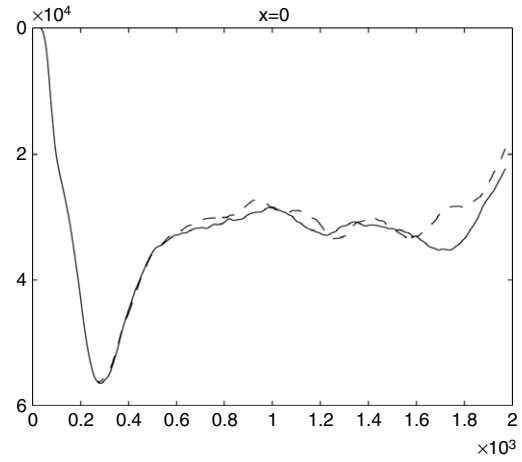

(a) Displacement of DE under the impactor.

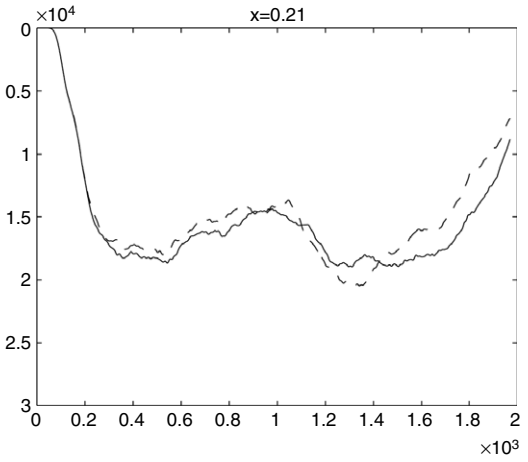

(b) Displacement of DE at 0.21 m of the impact.

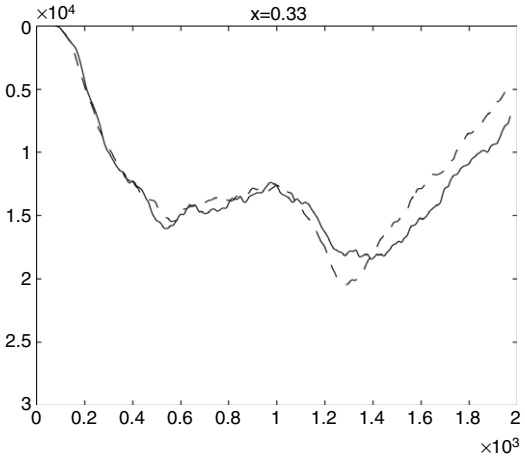

(c) Displacement of DE at 0.33 m of the impact.

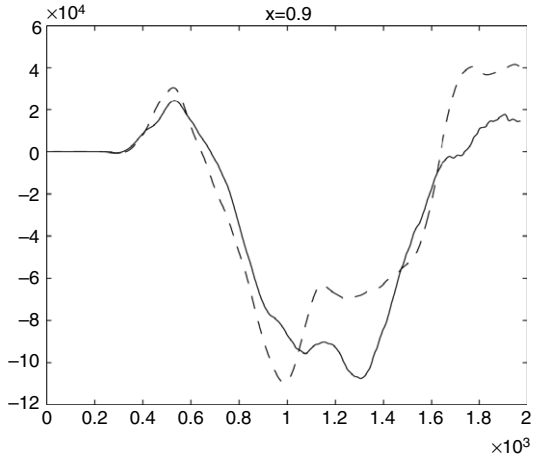

(d) DE displacement compares to FE displacement at 1 m of the impact.

Fig. 9. Comparison of displacement between only DE model (full line) and coupled DE/FE model (dotted line).

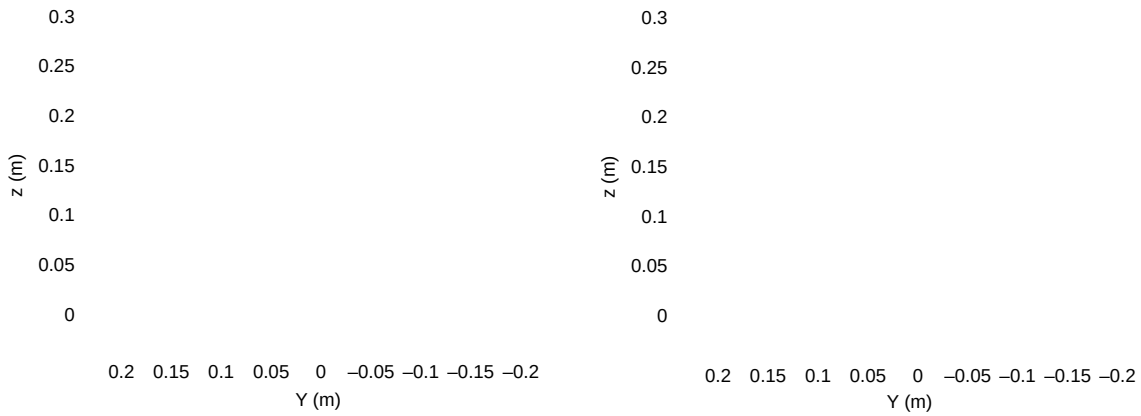

Fig. 10. Comparison of damage response between the full DE model (left) and coupled model (right).

Table 1
Comparison of the duration of the simulation.

Model	DE	Coupled DE/FE
Number of DE	120 808	6588
Number of FE node	0	5935
n_b (FE layer in bridging domain)		3
Number of time step	100 000	100 000
Duration of computation	42 h 50 min	3 h 39 min

with the full DE approach and the coupled DE/FE model are compared at the same time. In this figure, the damage is evaluated as the ratio between broken links and initial links. Damage is proportional to the sphere darkness. Black color corresponds to free DE, the lightest DE have no broken links.

One of the aims of this combined FE/DE modelling is to use the efficiency of the DE fracturing process on a large structural scale. This has been possible by reducing both the number of DE and the computation time. The analysis of computation times for this problem shows that the coupled FE/DE model is ten times faster than the full DE model (Table 1).

This difference on the computation time comes from the ration of DE in the full DE model, and the DE in the coupled model. This coupled method can easily use a multi-time step algorithm to further improve the computational time. The computation time in the FE model is negligible. By reducing the time of simulation, we can manage to simulate a larger or more complex structure and/or refine the discretization.

6. Conclusion

The proposed coupled method is able to simulate an impact on a concrete structure. The domain is divided into two models, DE or FE, depending on characteristic wave lengths of dynamic phenomena that are essential for a correct prediction of damage. The coupling is based on a Lagrange multipliers approach, but numerical modifications are introduced in order to reduce the spurious reflections. The reduction of Lagrange multipliers by means of a relaxation parameter introduces temporal freedom on DE nodes in the bridging domain, and the reflection is then attenuated. The relaxation parameter method, added to diagonal matrices of Lagrange multipliers, is a very efficient way to get a correct prediction of damage in the DE subdomain without spurious phenomena. Moreover, this method reduces the time necessary to compute Lagrange multipliers and, globally, the computation is faster.

This computation time reduction, obtained with the proposed coupled approach, allows us to carry out 3D simulations of very large structures under impact and, locally, a real description of the media can be modelled at a satisfying scale.

Acknowledgments

The authors would like to thank the R&D Division of France's EDF electric utility company for financial support, especially Sergueï Potapov for giving advice.

References

[1] Bathe KJ, Walczak J, Welch A, Mistry N. Nonlinear analysis of concrete structures. Comput Struct 1989;32(3/4):563–90.
[2] Cundall PA, Strack ODL. A discrete numerical model for granular assemblies. Geotechnique 1979;29(1):47–65.
[3] D'addeta GA, Kun F, Ramm E. On the application of the discrete model to fracture propagation in concrete. Granulat Matter 2002;4:77–90.
[4] Camborde F, Mariotti FC, Donzé FV. Numerical study of rock and concrete behaviour by discrete element modelling. Comput Geotechnics 2000;27:225–47.
[5] Rousseau J, Frangin E, Marin P, Daudeville L. Damage prediction in the vicinity of an impact on a concrete structure: A combined FEM/DEM approach. Comput Concrete 2008;5(4):343–58.
[6] Li S, Liu WK. Meshfree particle methods. Springer; 2004.
[7] Rabczuk T, Xiao SP, Sauer M. Coupling of mesh-free methods with finite elements: Basic concepts and tests results. Commun Numer Meth Eng 2006;22(10):1031–65.
[8] Azevedo NM, Lemos J. Hybrid discrete element/finite element method for fracture analysis. Comput Meth Appl Mech Eng 2006;195(33–36):4579–93.
[9] Cusatis G, Bazant ZP, Cedolin L. Confinement-shear lattice CSL model for fracture propagation in concrete. Comput Meth Appl Mech Eng 2006;195:7154–71.
[10] Onate E, Rojek J. Combination of discrete element and finite element method for dynamics analysis of geomechanics problems. Comput Meth Appl Mech Eng 2004;193:3087–128.
[11] Bicanic N, Munjiza A, Owen DRJ, Petrinic N. From continua to discontinua — A combined finite element/discrete elementmodelling in civil engineering. Dynamic Modelling of Geomaterials, ALERT geomaterials. 1997.
[12] Xiao S, Belytschko T. A bridging domain method for coupling continua with molecular dynamics. Comput Meth Appl Mech Eng 2004;193:1645–69.
[13] Ben Dhia H, Rateau G. The Arlequin method as a flexible engineering design tool. Int J Numer Meth Eng 2005;62:1442–62.
[14] Berriaud C, Sokolovsky A, Gueraud R, Dulac J, Labrot R. Comportement local des enceintes en béton sous l'impact d'un projectile rigide. Nucl Eng Des 1978;45:457–69.
[15] 1993 CEB-FIP model code 1990. Comité Euro-international du Béton, trowbridge. Wiltshire (UK): Redwood Books; 1993.
[16] Nachtsheim W, Stangenberg F. Interpretation of results of Meppen slab test — Comparison with parametric investigations. Nucl Eng Des 1982;75:283–90.
[17] Sugano T, Tsubota H, Kasai Y, Koshika N, Itoh C, Shirai K, et al. Local damage to reinforced concrete structures caused by impact of aircraft engine missiles. Nucl Eng Des 1993;140:387–423.
[18] Camborde F, Grillon Y, Chaigneau F. Discrete Element Method for predicting the behaviour of concrete under dynamic loading. J de physique IV 2000;10(9):467–74.
[19] Hentz S, Daudeville L, Donzé FV. Discrete Element Modelling of concrete submitted to dynamic loading at high strain rates. Comput Struct 2004;82:2509–24.
[20] Donzé FV, Magnier SA, Daudeville L, Mariotti C, Davenne L. Numerical study of compressive Behaviour of concrete at high strain rates. J Eng Mech 1999;125(10):1154–63.
[21] Hentz S, Daudeville L, Donze FV. Identification and validation of a discrete element model for concrete. J Eng Mech 2004;130:709–19.